Two Phase (Reconfigurable) Inverting Switched Capacitor Converter for Micro Power Applications and Its Accurate Equivalent Resistance Calculation

Vivekanandan Subburaj, *Student Member, IEEE*, Yerzhan Mustafa, *Student Member, IEEE*, Ainur Zhaikhan, Debashisha Jena, *Senior Member, IEEE*, Parthiban Perumal, *Senior Member, IEEE*, and Alex Ruderman, *Senior Member, IEEE*

***Abstract*—This brief addresses inverting switched capacitor converter (SCC) for driving the white light emitting diodes (WLEDs). The various voltage conversion ratios (VCRs) are selected to control the WLEDs blacklights, which helps to save the battery life. The major contribution are developing maximum VCRs for power converter integrated circuits (ICs) and equivalent resistance (R_{eq}) accurate calculation which includes all conduction and ohmic losses. Furthermore, inverting SCC (ISCC) experimental results are obtained from prototype model. Accurate R_{eq} analyses validates the accuracy of proposed topology. It is designed for low voltage of 10 mV to 0.1 V and it provides the output voltage of −100 mV to −0.5 V. Finally, the novelty of accurate R_{eq} calculation in this brief is that the calculation results are verified with experimental ones, particularly, at the transition region (between slow switching limit and fast switching limit). On the other hand, calculation, simulation and experimental results perfectly coincide with each other. Accurate equivalent resistance calculation and average current calculation are compared and some of the recent publications providing the merits of the proposed converter are explained.**

***Index Terms*—Inverting SCC, WLEDs, accurate equivalent resistance, voltage ratios, Fibonacci, negative.**

I. Introduction

INVERTING switched capacitor converters (ISCC) are used to control the blacklights of white light emitting diodes (LEDs) [1]. Switched capacitor converter (SCC) is a low power DC-DC circuit, which is used to generate a positive or negative buck or boost voltage. In some applications, SCC acts as a voltage regulator or low drop out (LDO) regulator. White LEDs (WLEDs) [1] provide ideal blacklight color display for cellular phones and electronic displays. The WLED drivers can be implemented either by using switched-inductor converter or switched-capacitor converter (SCC). Obviously, the switched-inductor converter provides high efficiency, but at the same time the inductors are bulky which makes them unfavorable for on-chip implementation [2]. In contrast, SCC provides less size, low cost and less battery usage for all low power applications.

ISCC are used for cellular phones to dim a display after few seconds of usage. Also, these converters need to maintain high efficiency in low-light condition to prevent fast-draining of the battery. There are a few ISCCs available commercially. For example, TLC555-Q1 converter, which is developed by Texas Instruments, is used to control the reverse battery voltage protection. In fact, a normal diode can be used for controlling the reverse flow, but it causes lower efficiency and voltage drop. Similarly, LTC3260 is designed for both positive and negative charge pump, and also used for biomedical applications and portable equipments. Recently, MAXIM designed a negative voltage doubler (MAX1681) using three external capacitors.

Moreover, MAXIM designed a variable negative voltage regulator (MAX1673) with minimum voltage ratios and it is designed by fixed frequency control. Similarly, MAX1673 negative converters can provide maximum of two voltage ratios. Shin *et al.* [3] explains negative DC-DC converter for driving the organic LEDs (OLEDs) using capacitors and magnetic components with less VCRs and equivalent resistance (R_{eq}) is not calculated. On the other hand, Mahnashi and Peng [4] discusses the negative ratios using SCC with multiple input and multiple output but R_{eq} for the proposed circuit is not considered. Therefore, ISCC is employed in this brief which is able to generate 7 voltage conversion ratios (VCRs) using 10 switches and 3 capacitors. This brief addresses theoretical aspects of power management integrated circuit (IC) modelling. The modelling and experimental setup was performed and validated. Only the IC fabrication (chip design) of the same topology converter is left for future work. The main contribution of this brief is development of negative voltage converter for micro power applications. The standard Fibonacci topology is feasible for generating maximum voltage ratios and provides high efficiency with two phase switching. On the other hand, generation of negative voltage ratios using the same topology is difficult because the

Manuscript received July 14, 2018; revised October 11, 2018; accepted November 25, 2018. Date of publication December 19, 2018; date of current version July 30, 2019. This brief was recommended by Associate Editor Y.-M. Chen. *(Corresponding author: Ainur Zhaikhan.)*

V. Subburaj, D. Jena, and P. Perumal are with the Department of Electrical and Electronics Engineering, National Institute of Technology Karnataka, Surathkal 575025, India (e-mail: vivek-ee14f11@nitk.edu.in; bapu4002@gmail.com; parthdee@nitk.edu.in).

Y. Mustafa, A. Zhaikhan, and A. Ruderman are with the Department of Electrical and Computer Engineering, Nazarbayev University, Astana 010000, Kazakhstan (e-mail: yerzhan.mustafa@nu.edu.kz; ainur.zhaikhan@nu.edu.kz; alexander.ruderman@nu.edu.kz).

Color versions of one or more of the figures in this paper are available online at http://ieeexplore.ieee.org.

Digital Object Identifier 10.1109/TCSII.2018.2886076

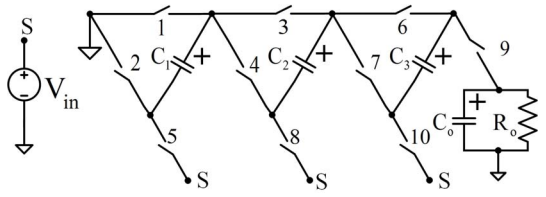

Fig. 1. Proposed circuit implementation of ISCC.

TABLE I
NEGATIVE VCRS

VCRs	Switches									
	1	2	3	4	5	6	7	8	9	10
$-2 * V_{in}$	ϕ_1	ϕ_2	ϕ_2	ϕ_1	ϕ_1	ϕ_1	-	ϕ_2	ϕ_1	-
$-3 * V_{in}$	ϕ_1	ϕ_2	ϕ_1	ϕ_2	ϕ_1	ϕ_1	ϕ_2	ϕ_1	ϕ_2	ϕ_1

whole design needs to be reconfigured. Therefore, the chip size varies and capacitor placement needs to be changed accordingly. Finally, it provides low efficiency and also the size of electronic gadgets is large.

Commonly, SCCs are characterized by equivalent resistance. Equivalent resistance is a concept introduced to describe power losses through SCC. Power dissipation in all resistive elements of the circuit is modeled as a loss in some R_{eq} due to average load current passing through it.

II. INVERTED SCC

ISCC plays a vital role in micro power electronics devices. It is mainly used for driving the WLEDs black-lights in different voltage conditions. The ISCC circuit is depicted in Fig. 1. ISCC is developed using general Fibonacci schematic [5] using 10 bidirectional switches and three flying capacitors. The proposed ISCC generates 7 VCRs [4], ($-1/2V_{in}$, $-1/3V_{in}$, $-1/4V_{in}$, $-1V_{in}$, $-2V_{in}$, $-3V_{in}$ and $-4V_{in}$) and the switching sequence of the VCRs are shown in Table I. Two phases, ϕ_1 and ϕ_2, are used for driving the bidirectional switches (1 to 10). ϕ_1 and ϕ_2 are 50% duty cycle non-overlapping clocks, where ϕ_1 is considered as the charging phase and ϕ_2 is the discharging phase. The VCR of the negative outputs [4] can be quantified as following:

$$\frac{V_{in}}{V_o} = -\frac{P}{Q}; \quad 1 \leq max|P, Q| < F_{i+2}, \tag{1}$$

where P and Q follow Fibonacci series, and F_i is a Fibonacci number. The flying capacitors (C_1 to C_3) are charged through negative terminal and discharged via positive terminal to generate negative VCRs. For each VCRs, individual gating is chosen and used to generate the signals for controlling the bidirectional switches. For the simplicity, $-2V_{in}$ VCR is considered for designing the converter and calculating the corresponding R_{eq}. The switches 2, 3 and 8 are connected to charge the flying capacitors in negative directions (Phase 2) and discharge (Phase 1) using 1, 4, 5, 6 and 9. Equivalent circuit of ISCC for both Phase 1 and Phase 2 are depicted in Fig. 3. Accurate calculations for both phases are discussed in the following Sections.

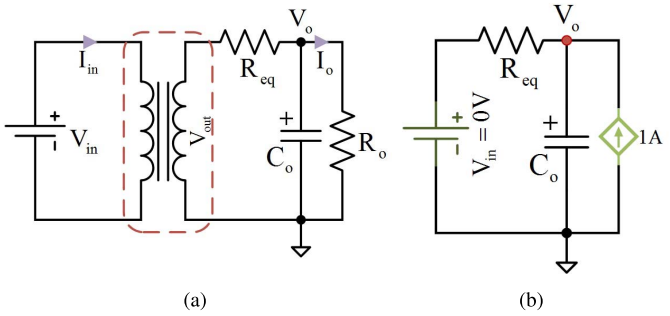

(a) (b)

Fig. 2. (a) ISCC model [7]; (b) Validation model of R_{eq} [6].

III. EQUIVALENT RESISTANCE, R_{eq}

R_{eq} is helpful for SCC to calculate conduction and ohmic losses in semiconductor components used in proposed ISCC. Kushnerov [5] explains the equivalent circuit model of ISCC for an average output voltage ($V_{out} = -n * V_{in}$) where, n is the target ratio and V_{in} is the input voltage, which is shown in Fig. 2(a). Simple way to understand the measurement of R_{eq} [6] consists in connecting the current source at load and setting the input DC source to 0 V as depicted in Fig. 2(b). Finally, connect the probe to measure the average output voltage across output capacitor as shown in Fig. 2(b). Abraham *et al.* [2] explained the analysis of R_{eq} in basic circuit theory concept using first order RC network. If the switching frequency is low, the associated time period is large, then, the flying capacitor may be fully charged and discharged, the first case is called the slow switching limit (SSL). On the contrary, if the switching frequency is high, then the time period is small and consequently, the flying capacitor cannot be completely charged, this second case is said to be the fast switching limit (FSL) mode [7], [8]. R_{eq} analysis is studied by many researchers [5], [7]–[9] but assuming infinite filter capacitances, they provided approximate results. The most popular Seeman [8], who derived the R_{eq} formula is given by,

$$R_{eq} = \left[(R_{SSL})^2 + (R_{FSL})^2\right]^{1/2}. \tag{2}$$

where R_{FSL} and R_{SSL} are fast switching and slow switching R_{eq}. On the other hand, Makowski [10] explains another formula for R_{eq}, is given by,

$$R_{eq} = \left[(R_{SSL})^{2.545} + (R_{FSL})^{2.545}\right]^{1/2.545}. \tag{3}$$

According to equation (2) and (3), R_{eq} calculations are approximate. To overcome these issue, accurate equivalent resistance is calculated and it is validated using ISCC.

Kushnerov [5] explains to identify the charge flow equation on SCC on each switching intervals. The steps to be followed for generating linear equation:

1) Consider steady state value as zero.
2) Apply Kirchoff current law (KCL).
3) Total charge is added and equate to linear equations.

According to Kushernov's solution in [5] charge balance equations define a relation in magnitude between the charges flowing during each phase. The last one defines their absolute

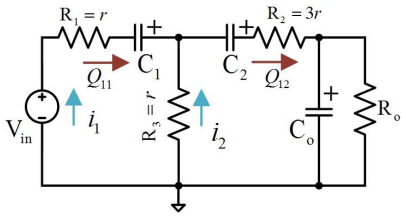

(a) Phase 1 (ϕ_1)

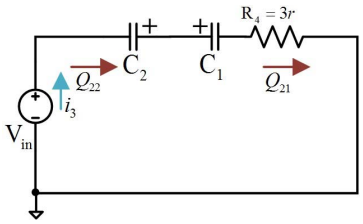

(b) Phase 2 (ϕ_2)

Fig. 3. Equivalent circuit of proposed converter for -2V_{in} VCR.

value (scale) based on the net charge supplied to the load. Kushnerov's method [5] finds accurate equivalent resistance by computing average phase currents in terms of load current, based on the charge balance equations. However, this approach was applicable only for the first order RC circuits.

Accurate R_{eq} method that can deal with higher order RC circuits was proposed by Mustafa *et al.* [11]. In this method, R_{eq} is calculated by using the charge balance and partial KVL equations.

To analyse the ISCC, assumptions are to be considered as explained in [11]. High order RC circuit are used for each switching phase. ISCC charged capacitors are determined by solving linear algebraic equation. Calculation of overall losses can be solved by considering the exponential currents in the circuit and then by successively: measuring squared current in the given time intervals and computing R_{eq}. The comparison between R_{eq} methods [8], [10], [11] is made in Section VI.

IV. Detailed Accurate Equivalent Resistance Calculation

Accurate equivalent resistance calculations are derived using charge flow balance equations using Fig. 3 as given below,

$$Q_{21} - Q_{11} = 0; \tag{4}$$

$$Q_{22} + Q_{12} = 0; \tag{5}$$

$$Q_{12} = Q, \tag{6}$$

where Q - net charge delivered to the load. By solving the (4)–(6) charge flow solution is given by,

$$Q_{11} = Q_{21} = Q_{22} = -Q; \quad Q_{12} = Q. \tag{7}$$

For accurate calculation, equal switch resistances (r) and switched capacitances (C) are considered. Capacitor ESR was not considered in calculations, based on the requirement, ESR can be included. Phase 1 (Fig. 3(a)) is the 2nd order circuit that has two time constants (T_1 and T_2). Phase 2 (Fig. 3(b)) has only series connections that correspond to the 1st order circuit with one time constant (T_3) where the time constants T_1, T_2 and T_3 are given by,

$$T_1 = 1.59rC; \quad T_2 = 4.41rC; \quad T_3 = (3/2)rC. \tag{8}$$

Following the methodology in [11] for Phase 1 and methodology in [5] for Phase 2, the equivalent resistance (R_{eq}) of ISCC can be calculated.

A. Phase 1 Capacitor Currents

In order to find 4 unknown coefficients of Phase 1 capacitor currents (9), (10), a set of 4 linear equations are developed as given in (11), (12),

$$i_1(t) = a_{11}e^{-t/T_1} + a_{12}e^{-t/T_2}; \tag{9}$$

$$i_2(t) = a_{21}e^{-t/T_1} + a_{22}e^{-t/T_2}, \tag{10}$$

where three equations are developed using capacitor charge flow methodology as explained in (11). The other two equations are developed from partial KVL method which is explained in (12) using Fig. 3(a).

$$\int_0^{T/2} i_1(t)dt = -\int_0^{T/2} (i_1(t) + i_2(t))dt = -Q; \tag{11}$$

$$i_1(t)r + \frac{1}{C}\int_0^{T/2} i_1(t)dt = i_2(t)r, \tag{12}$$

where T is a switching period.

B. Phase 2 Capacitor Current

To find unknown coefficient of Phase 2 capacitor current (13), one equation (14) is sufficient from charge flow methodology and it is derived using Fig. 3(b) that is given by,

$$i_3(t) = Ae^{-t/T_3}; \tag{13}$$

$$\int_0^{T/2} i_3(t)dt = -Q. \tag{14}$$

R_{eq} that is calculated by finding power loss (squared currents integrals) on each segment is given by,

$$R_{eq} = \frac{1}{Cf}\coth\left(\frac{1}{6rCf}\right) + \frac{1}{6.83Cf}\coth\left(\frac{1}{6.34rCf}\right) + \frac{1}{1.17Cf}\coth\left(\frac{1}{17.66rCf}\right), \tag{15}$$

where f is the switching frequency. The first term of expression (15) corresponds to Phase 2, while the last two terms concern Phase 1 (one for each time constant).

V. Experimental Verification and Discussion

This is the model for developing a on-chip ISCC. This experimental setup was verified by designing the converter using electrical components. The proposed converter is validated using MAX4567 switches [2] with turn-on resistance (r) of 0.3 Ω. For the capacitors, 22 μF flying capacitors and 220 μF output capacitor are used, with ESR equals to 100 mΩ. To drive the backlight WLEDs, minimum output voltage

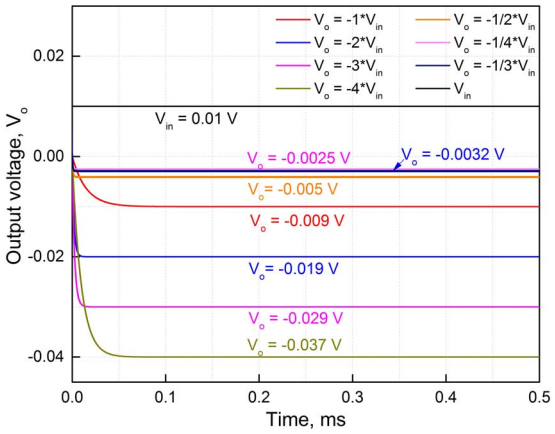

(a)

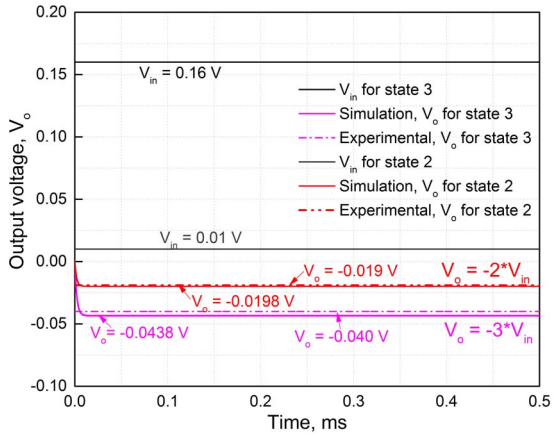

(b)

Fig. 4. Simulation results of ISCC: (a) V_o time response for all VCRs; (b) Comparison between Experiment and Simulation results for -2V_{in} and -3V_{in} VCRs.

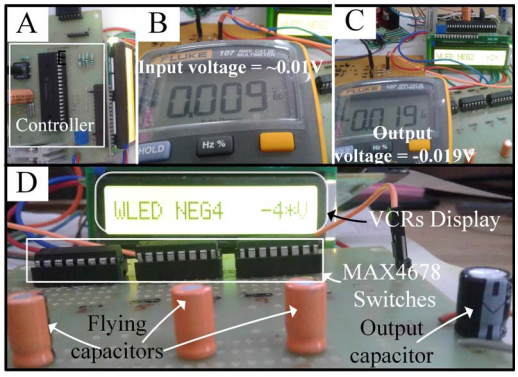

Fig. 5. Experimental setup of the proposed ISCC.

needs to be 800 mV. But the MAX4567 switch can be vary from 10 V to −50 mV (single source). In this brief, for simplicity and validation of the converter VCRs the prototype model is implemented using the input voltage ≈0.01 V. It is generated using voltage divider circuit and its losses are not considered for the analysis. On the other hand, according to requirement ESR is easy to include for analysis but in this analysis, ESR is not considered. Simulation results of all ISCC VCRs are shown in Fig. 4(a). Experimental results for

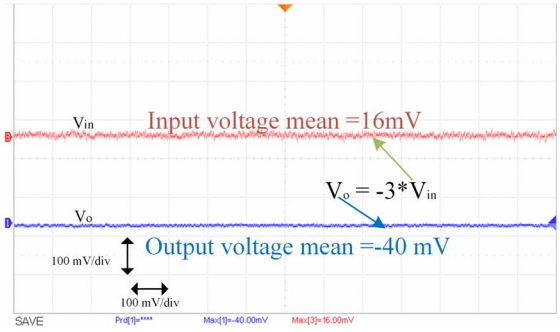

Fig. 6. Experimental results of $-3V_{in}$ when R_o is 1 kΩ.

TABLE II
COMPARISON WITH DIFFERENT ISCC AND R_{eq} ANALYSIS

Parameters	[3]	[4]	[5]	This work
VCR	-	4	19	7
Voltage ratios	-	Negative	Positive	Both
V_{in}	1.8 V	1 V	1 V to 8 V	10 mV – 0.5V
V_o	-4 V	-1, 1, 2	Variable	-100 mV – -1.5 V
f	0.5 MHz	500 kHz	NA	50 – 100 kHz
Flying capacitors	NA	2	3	3
R_{eq} Analysis	NA	NA	Approximate	Accurate
R_o	NA	NA	500 Ω – 5 kΩ	1 kΩ – 1 MΩ
Efficiency	81.9%	NA	90%-95%	85-95%

two different input and different VCRs are shown in Fig. 4(b). From Fig. 4(b) simulation and experimental results are in good agreement to each other even in larger load conditions. The switching controller for ISCC CMOS bidirectional switches is depicted in Fig. 5. Experimental results for $(-2V_{in})$ is shown in Fig. 5. B and Fig. 5. C where the input voltage is ≈0.01 V and the output voltage −0.019 V. Fig. 5. D shows the overall prototype of proposed ISCC. On the other hand, tests were also performed for $-3V_{in}$. The corresponding experimental results are shown in Fig. 6 where the input voltage for this particular VCR is 16 mV and the output voltage is −40 mV. Comparison of all VCRs model, simulated and hardware results are discussed in Fig. 7(a). Fig. 7(b) shows a comparative study and a discussion between: accurate R_{eq} analysis, simulation and experimental results. The conditions were identical with the 3 approaches: ESR of 0.1 Ω and $R_o = 1$ kΩ. From Fig. 7(b), we conclude the ISCC accurate R_{eq}, the simulation R_{eq} and the experimental R_{eq} are in good agreement. Finally, comparison results of recent work related to ISCC are discussed in Table II.

VI. COMPARISON WITH ACCURATE AND APPROXIMATE ISCC R_{eq} ANALYSIS

Equivalent resistance is calculated for each method and discussed in this Section. The equivalent resistance of accurate calculation is derived in Section IV and the final R_{eq} equation is given in (15). Approximate R_{eq} using SSL and FSL solution is given in (16),

$$R_{SSL} = 2/(Cf); \quad R_{FSL} = 22r. \tag{16}$$

Seeman [8] and Makowski [10] approximate equations for ISCC are discussed in Section III equation (2) and (3). Comparison result of accurate and approximate method of

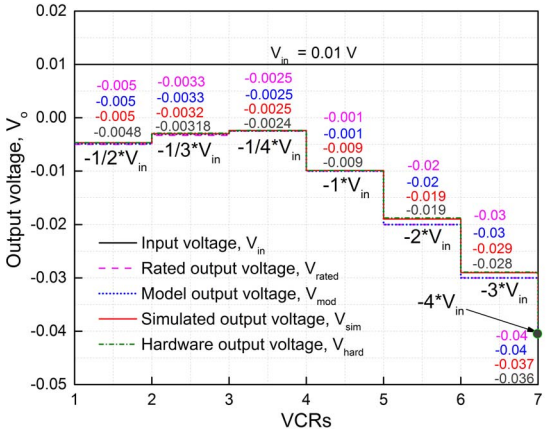

(a) Comparison of modeled, simulated and experimental results

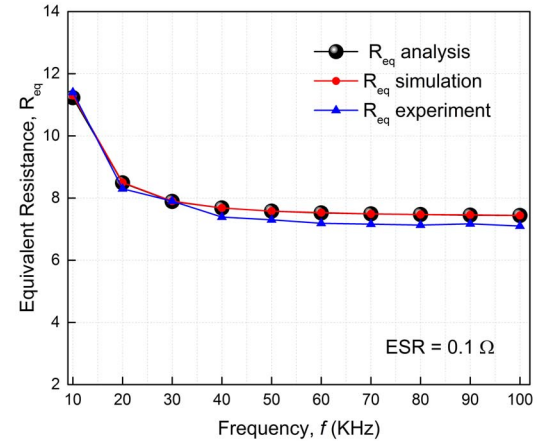

(b) Comparison between accurate R_{eq} analysis, experimental and simulation results for -2V_{in} VCR

Fig. 7. Comparison between results for ISCC.

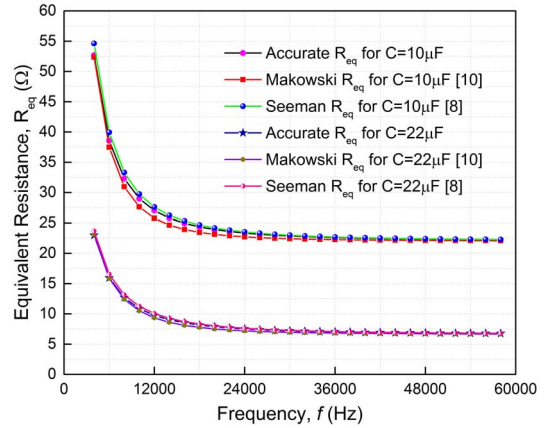

Fig. 8. Comparison of ISCC accurate R_{eq} with Seeman [8] and Makowski [10].

ISCC is depicted in Fig. 8. Two cases are plotted in the Fig. 8. One is for equal flying capacitances C = 10 μF and switch resistances r = 1 Ω. Similarly, experimental data are compared and plotted for equal flying capacitances C = 22 μF and switch resistances r = 0.3 Ω. It should be noted that approximate equivalent resistance calculation coincides with the accurate one only in the FSL and SSL regions. However, in the transition region the difference is considerable as shown in Fig. 8. The recent finding of accurate equivalent resistance calculation [11] shows that there is no need to calculate FSL and SSL separately. Therefore, there is more elegant way to accurately calculate equivalent resistance over the whole switching interval by using the approach proposed in [11].

VII. Conclusion

In this brief, the working concept of the ISCC which are mostly used in micro power applications are analysed and verified experimentally. Compare to all ISCC methods proposed ISCC provides high efficiency and maximum voltage ratios. ISCC is designed for three stage converter using ten switches and three flying capacitors which generates seven voltage ratios. It achieves 95% peak efficiency where the losses are not considered. Further, the accurate equivalent resistance analysis of ISCC includes ohmic and conduction losses, which are analysed and validated using experimental setup. The proposed ISCC shows good results in theoretical, simulation and experimental validations. The accurate equivalent resistance calculation and simulation results are almost overlapping. Finally, accurate equivalent resistance calculation which is validated for ISCC are compared with two approximate methods suggested by Seeman and Makowski. Comparison shows that for the range of frequencies between SSL and FSL those two methods can be not enough accurate for modeling losses of SCC.

References

[1] C. Richardson, *LED Applications and Driving Techniques*, Nat. Semicond. Corporat., Santa Clara, CA, USA, 2007. [Online]. Available: www.national.com/onlineseminar/2007/led/national_LEDseminar.pdf

[2] C. Abraham *et al.*, "Reconfigurable highly efficient CMOS-based dual input variable output switched capacitor converter for low power applications," *Electron. Lett.*, vol. 54, no. 2, pp. 89–91, Jan. 2018.

[3] S.-H. Shin, S.-K. Hong, and O.-K. Kwon, "High-efficient inverting buck-boost converter with fully digital-controlled switch width modulation for microdisplays," *Electron. Lett.*, vol. 54, no. 5, pp. 309–311, Mar. 2018.

[4] Y. Mahnashi and F. Z. Peng, "Generalization of the fundamental limit theory in a switched-capacitor converter," *IEEE Trans. Power Electron.*, vol. 32, no. 9, pp. 6673–6676, Sep. 2017.

[5] A. Kushnerov, "Multiphase Fibonacci switched capacitor converters," *IEEE J. Emerg. Sel. Topics Power Electron.*, vol. 2, no. 3, pp. 460–465, Sep. 2014.

[6] A. Zhaikhan, V. Subburaj, D. Jena, P. Perumal, and A. Ruderman, "Design, modeling and analysis of a new dual input-output switched capacitor converter," in *Proc. TENCON IEEE Region 10 Conf.*, Penang, Malaysia, 2017, pp. 673–677.

[7] M. Evzelman and S. Ben-Yaakov, "Average-current-based conduction losses model of switched capacitor converters," *IEEE Trans. Power Electron.*, vol. 28, no. 7, pp. 3341–3352, Jul. 2013.

[8] M. D. Seeman, "A design methodology for switched-capacitor DC–DC converters," Dept. Elect. Eng. Comput. Sci., Univ. California at Berkeley, Berkeley, CA, USA, Rep. UCB/EECS-2009-78, 2009.

[9] A. Junussov and A. Ruderman, "Analysis of a reconfigurable Fibonacci switched capacitor converter with a multiphase balanced switching," in *Proc. IEEE 5th Int. Conf. Power Eng. Energy Elect. Drives (POWERENG)*, Riga, Latvia, 2015, pp. 164–169.

[10] M. S. Makowski, "A note on resistive models of switched-capacitor DC–DC converters: Unified incremental-graph-based formulas given," in *Proc. Int. Conf. Signals Electron. Syst. (ICSES)*, Wrocław, Poland, 2012, pp. 1–4.

[11] Y. Mustafa, A. Zhaikhan, and A. Ruderman, "SCC Equivalent Resistance: The relationship for complementary buck and boost and accurate calculation for 2-phase converters," in *Proc. IEEE 18th Int. Power Electron. Motion Control Conf. (PEMC)*, Budapest, Hungary, 2018, pp. 188–193.